Combination of cycling hyperthermia and Echinacoside creates synergistic curing effect on pancreatic cancer PANC-1 cells

Wei-Ting Chen[1,2¶], You-Ming Chen[2,3¶], Guan-Bo Lin[1,2], Yu-Yi Kuo[1,2], Hsu-Hsiang Liu[2,3], and Chih-Yu Chao[1,2,3,*]

[1] Department of Physics, Lab for Medical Physics and Biomedical Engineering, National Taiwan University, Taipei 106319, Taiwan

[2] Molecular Imaging Center, National Taiwan University, Taipei 100233, Taiwan

[3] Graduate Institute of Applied Physics, Biophysics Division, National Taiwan University, Taipei 106319, Taiwan

[¶] These authors contributed equally to this work.

* Corresponding author

E-mail: cychao@phys.ntu.edu.tw (CYC)

Keywords: combination treatment, synergistic effect, hyperthermia, pancreatic cancer, DNA damage

Abstract

Therapy targeting the suppression of human MutT homolog 1 (MTH1) has been gaining ground in recent years, thanks to its resulting significant increase of 8-hydroxy-2'-deoxyguanosine triphosphate (8-oxo-dGTP) accumulation in genomic DNA, causing DNA damage and apoptotic cell death. Echinacoside (Ech), a natural phenylethanoid glycoside first extracted from Echinacea angustifolia or desert plant Cistanches is one of a few natural products which are capable of inhibiting the MTH1 function. It, however, is difficult to apply it in clinical trials, due to high cost for effective dosage in need. In the study, we show that combination with thermal-cycling hyperthermia (TC-HT), a novel physical treatment, can amplify the curative effect of Ech, reducing its dosage in need significantly. The combination resulted in a multipronged mechanism targeting multiple key apoptotic regulating proteins such as Bcl-2 and MAPK family proteins. Its effect is expected to be comparable to the treatment strategy containing MTH1, Bcl-2, and ERK inhibitors, posing as new promising approach in cancer treatment.

38 # Introduction

39 Due to difficulty in early diagnosis, pancreatic cancer has remained a highly fatal
40 disease with a five-year survival rate less than 10% in the U.S., and is predicted to be
41 the second leading cause for cancer-related death in the next decade in Western
42 countries. Despite progress in diagnosis and therapy, prognosis for pancreatic cancer
43 patients has remained poor. Given the imperative need for progress in early diagnosis
44 and therapeutic effect, it is worthwhile to seek novel anticancer agents and alternative
45 therapies, in order to improve the life quality of pancreatic cancer patients.

46 Ingredients extracted from plants or traditional Chinese herbs, known as
47 phytochemicals, have emerged as promising novel anticancer drug sources, on top of
48 their application in anti-virus, anti-cancer and anti-inflammatory therapies [1-4]. A
49 main reason for growing popularity of herbal drugs is their absence of side effects.
50 Experiments have shown that anticancer phytochemicals attain curative effect via
51 regulating molecular pathways implicated in proliferation and progression of cancer
52 cells. A noticeable example is Echinacoside (Ech), a natural phenylethanoid glycoside
53 extracted from Echinacea angustifolia or desert plant Cistanches. Ech has been proven
54 to be capable of rescuing the PC-12 neuronal cells from neurotoxicity via attenuating
55 mitochondrial dysfunction and inflammatory responses by reducing ROS production
56 [5]. Recent studies have also shown that Ech can improve the behavioral disorders in
57 mouse model with Parkinson's disease [6]. Besides, the hepatoprotection and anti-
58 senescence effects of Ech have also been found in mouse models [7]. However, the
59 specific mechanism responsible for Ech's anticancer effect remains unknown, as only
60 a few cancer cell lines have been studied [8-10].

61 Recent studies have manifested that Ech is capable of inhibiting the catalytic
62 activities of MutT homolog 1 (MTH1), a protein responsible for sanitizing oxidized

63 deoxynucleoside triphosphate (dNTP), highly expressive in various cancer cells [11].
64 According to recent studies [12, 13], MTH1 also plays a key role in the survival of
65 cancer cells, helping them to avoid incorporation of oxidized dNTPs, which cause DNA
66 damage and cell death. Noticeably, the inhibition of MTH1 doesn't affect the growth
67 and survival of normal cells [14], underscoring the potential of such therapeutic
68 approach. Some MTH1 inhibitors have been developed with the aim of suppressing
69 cancer growth by damaging DNA in cancer cells [15]. In the study, we aimed to explore
70 the anticancer effect of combining Ech with thermal treatment and the underlying
71 mechanism.

72 As an adjuvant therapy, Hyperthermia (HT) has been applied along with radiation
73 or chemotherapy attaining synergistic curative effect for cancer patients [16]. However,
74 heat generated by continuous HT therapy may damage normal cells and cause other
75 side effects, due to lack of precision and flexible control of heating temperatures and
76 parameters. To cope with the problem, our previous study proposed a novel thermal
77 therapy, namely thermal cycling hyperthermia (TC-HT), for the anticancer treatment in
78 pancreatic cancer cells [17, 18]. The TC-HT treatment, which features alternating
79 application of high and low temperatures in combination with administration of various
80 natural compounds, has significantly enhanced curative effect without harming normal
81 cells.

82 In this paper, the study proposes an innovate treatment for pancreatic PANC-1
83 cancer cells, combining the natural compound Ech and the physical stimulus TC-HT,
84 both of which are capable of inhibiting the growth of cancer cells with minimum injury
85 to normal cells. Our results showed that TC-HT alone can inhibit the expression level
86 of MTH-1 protein significantly. Moreover, the combined treatment with Ech
87 demonstrated remarkable synergistic effect on inhibition of the expression level of
88 MTH-1, with TC-HT amplifying Ech-induced apoptotic cell killing and thus reducing

89 its necessary dosage. The remarkable anticancer performance could be attributed to TC-
90 HT enhancing the pharmacological effect of Ech to inhibit MTH1 expression and cause
91 8-hydroxy-2'-deoxyguanosine triphosphate (8-oxo-dGTP) accumulation, thereby
92 resulting in DNA damage and cell apoptosis. The combination treatment of Ech and
93 TC-HT also significantly down-regulated ERK and Bcl-2 proteins, which are associated
94 with cell proliferation and survival. The approach, thus, can attain an anticancer effect
95 comparable to chemotherapy drugs with minimum damage to normal cells, shedding
96 light on the potential of other combination therapies.
97

98 # Materials and methods

99 **Cell culture and treatment**

100 The human pancreatic cancer PANC-1 cell lines were purchased from the Bioresource
101 Collection and Research Center (BCRC, Hsinchu, Taiwan) and maintained in DMEM
102 (HyClone; Cytiva, Marlborough, MA, USA) supplemented with 10% fetal bovine
103 serum (HyClone; Cytiva) and 1% penicillin-streptomycin (Gibco; Thermo Fisher
104 Scientific, Inc., Waltham, MA, USA). H6c7 human pancreatic duct epithelial cell line
105 was obtained from Kerafast, Inc. (Kerafast, Inc.; Absolute Biotech, Boston, MA, USA)
106 and maintained in keratinocyte-serum free medium (Invitrogen; Thermo Fisher
107 Scientific, Inc., Carlsbad, CA, USA) supplemented with human recombinant epidermal
108 growth factor, bovine pituitary extract (Invitrogen; Thermo Fisher Scientific, Inc.), and
109 1% (v/v) penicillin and streptomycin. All cells were maintained in a humidified
110 incubator with 5% CO_2 and 95% air at 37˚C. Ech (Sigma-Aldrich; Merck KGaA,
111 Darmstadt, Germany) was dissolved in distilled water at a concentration of 2 mg/ml.
112 Cells were plated in 24-well plates or 3-cm culture dishes 24 h before treatment with or
113 without TC-HT and/or Ech. In the experiment, after Ech was added to cells, TC-HT

114 treatment was applied using the Thermal Cycler (Applied Biosystems; Thermo Fisher
115 Scientific, Inc., Waltham, MA, USA). The actual temperatures of cancer cells were
116 measured by a needle thermocouple located in the bottom of the well. After the
117 treatment, cells were incubated in a cell culture incubator until further analysis.
118
119 **Cell viability assay**
120 After the treatment, cell viability was determined by 3-(4,5-dimethylthiazol-2-yl)-2,5-
121 diphenyltetrazolium bromide (MTT) (Sigma-Aldrich; Merck KGaA) assay. The
122 medium was replaced with MTT solution (0.5 mg/ml in DMEM) and incubated at 37˚C
123 for 4 h. Then the supernatants were discarded, and the remaining formazan crystals
124 were dissolved with dimethyl sulfoxide and the optical density in each well was then
125 evaluated by the measurement of absorbance at 570 nm using an ELISA microplate
126 reader. The cell viability was calculated based on the optical intensity of the formazan,
127 and was expressed as a percentage of the untreated controls, which were set at 100%.
128
129 **Flow cytometric detection of apoptotic cells**
130 Apoptotic cells were examined using an Annexin V-FITC and propidium iodide (PI)
131 double-staining kit (BD Biosciences, Franklin Lakes, NJ, USA) by flow cytometry.
132 Cells used for flow cytometry were collected by trypsinization, washed twice with PBS,
133 and resuspended in binding buffer containing Annexin V-FITC and PI. Cells were
134 stained for 15 min at room temperature in the dark before being analyzed by flow
135 cytometry.
136
137 **ROS level detection**
138 Intracellular ROS levels were measured by flow cytometry using the fluorescent dye
139 dihydroethidium (DHE) (Sigma-Aldrich; Merck KGaA). PANC-1 cells were harvested

140 24 h after treatments and rinsed with PBS before staining. Cells used for flow cytometry
141 were collected by trypsinization and then incubated with 5 μM DHE for 30 min at 37˚C
142 in the dark. The fluorescence intensity emitted from DHE was measured by flow
143 cytometry, and the ROS levels were expressed as mean fluorescence intensity for
144 comparison.
145
146 **Measurement of intracellular 8-oxo-dGTP**
147 It is well known that Avidin binds with high specificity to 8-oxo-dGTP and used to
148 evaluate the incorporation of 8-oxo-dGTP into DNA. To observe cells under a confocal
149 microscope, they were seeded on coverslips. Cells treated with Ech and/or TC-HT on
150 coverslips were fixed with ice-cold methanol for 20 min followed by incubation in Tris-
151 buffered saline (TBS) with 0.1% Triton X-100 for 15 min. Cells were blocked in 15%
152 FBS, 0.1% Triton X-100 in TBS for 2 h at room temperature. Then, the cells were
153 probed with Alexa Fluor 488-conjugated Avidin (Alexa 488) (Invitrogen; Thermo
154 Fisher Scientific, Inc.) in blocking solution for 1 h at 37 °C. After washing with TBS
155 containing 0.1% Triton X-100 for three times, the coverslips were mounted on glass
156 slides in mounting medium with DAPI (Abcam, Cambridge, United Kingdom).
157 Fluorescent images were taken by a Zeiss LSM 880 inverted laser scanning confocal
158 microscope. These images were then analyzed with ImageJ v3.91 software to calculate
159 the relative fluorescence units (RFU) for both green and blue fluorescence. The level
160 of 8-oxo-dGTP in cells was determined by normalizing the RFU ratio of green (Alexa
161 488) to blue (DAPI) fluorescence against the control group.
162
163 **Western blot analysis**
164 The levels of protein expression in PANC-1 cells were examined by Western blot
165 analysis. After treatment with Ech or TC-HT or in combination, cells were scraped

166 from culture dishes and lysed in ice-cold RIPA lysis buffer containing protease inhibitor
167 (EMD Millipore, Billerica, MA, USA). The lysates were centrifuged at 12,000 × g for
168 30 min at 4˚C, and the supernatants were collected and the protein concentrations were
169 determined by Bradford protein assay (BioShop Canada Inc., Burlington, Canada).
170 Equal amount of proteins (30 μg) were resolved on 10% SDS-PAGE and then
171 transferred onto polyvinylidene fluoride membranes (EMD Millipore). Nonspecific
172 antibody binding sites were blocked in 5% nonfat milk in TBS with Tween-20 (TBST;
173 20 mM Tris-base, pH 7.6; 0.15 M NaCl; and 0.1% Tween-20) for 1 h at room
174 temperature. The blocked membranes were probed with MTH1, p-ERK, t-ERK, p-JNK,
175 Bcl-2, Bax, PARP (all from Cell Signaling Technology, Inc., Danvers, MA, USA) and
176 GAPDH (GeneTex, Inc., Irvine, CA, USA) antibodies overnight at 4˚C. The washed
177 membranes were then incubated with horseradish peroxidase-conjugated goat anti-
178 rabbit secondary antibodies (Jackson ImmunoResearch Laboratories, Inc., West Grove,
179 PA, USA) in a blocking solution. Immunoreactivity signal was visualized with an
180 enhanced chemiluminescence substrate (Advansta, Inc., Menlo Park, CA, USA) and
181 detected by the Amersham Imager 600 imaging system (GE Healthcare Life Sciences,
182 Chicago, IL, USA). Image analysis was performed with Image Lab software (Bio-Rad
183 Laboratories, Inc., Hercules, California, USA).
184
185 **Statistical analysis**
186 Statistical analyses were performed by using the OriginPro 2015 software (OriginLab).
187 The results were expressed as the mean ± standard deviation, and each data point
188 represented the average from three independent experiments. Differences of statistical
189 significance were determined by one-way ANOVA followed by Tukey's post-hoc test.
190 $P < 0.05$ was considered to indicate a statistically significant difference.
191

192 # Results

193 **TC-HT for in vitro application**

194 The detailed procedure of TC-HT treatment was described in our previous work [17].
195 Briefly, TC-HT was adopted to perform a thermal cycling treatment with a high
196 temperature period for 3 min and a cooling period for 30 sec, and this protocol was
197 repeated continuously for ten cycles. In the study, the temperature variation of the cells
198 under TC-HT was controlled by a modified PCR machine. The actual temperature in
199 the culture well was measured by a needle thermocouple. Fig 1 demonstrates the
200 temperature variation sensed by the cells at the bottom of the culture well during TC-
201 HT treatment.

202

203 **Fig 1. Temperature variation of TC-HT treatment.** The temperature was raised to a
204 desired high temperature for 3 min and decreased to a lower temperature for 30 s. The
205 high and low temperature periods of TC-HT were repeated continuously for ten times
206 in this study. The actual temperature in the culture well was monitored every 20 seconds
207 by a needle thermocouple.

208

209 **Ech and TC-HT synergistically suppress PANC-1 cell proliferation**

210 To examine the inhibitory effect of TC-HT and Ech, the viability of PANC-1 cells under
211 TC-HT and/or Ech administration was evaluated by the MTT assay. As shown in Fig
212 2A, Ech decreased the cell viability of PANC-1 cells in a concentration-dependent
213 manner. It was found that 20 μM Ech treatment on PANC-1 cells reduced the cell
214 viability to 80% compared to the control cells, which was used in the following
215 experiments. In this study, we aim to investigate the combination anticancer effect of
216 Ech and TC-HT, and thus low-dose Ech (20 μM) with mild inhibitory effect was

217 adopted in the combination treatment. The results also showed that TC-HT alone only
218 caused slight inhibitory effect as well as low-dose Ech. Moreover, we found that
219 combining TC-HT and Ech greatly decreased the viability of PANC-1 cells to only 29%
220 of the control group at the 20 μM low-dose Ech administration. Noteworthily, the
221 inhibitory effect of low-dose Ech (20 μM) in combination with TC-HT was close to that
222 of 100 μM Ech, indicating that the anticancer effect was highly amplified and therefore
223 the inhibitory concentration of Ech combined with TC-HT could be decreased to one
224 fifth of the Ech treatment alone. On the other hand, the H6c7 human pancreatic duct
225 epithelial cell line was treated with 20 μM Ech alone or in combination with TC-HT to
226 verify the toxic effect of the combination treatment on normal pancreatic cells. As
227 shown in Fig 2B, the combination treatment did not cause significant impact on the cell
228 viability of the H6c7 normal cells, while it exerted significant apoptotic cell death on
229 PANC-1 cancer cells in similar condition.
230
231 **Fig 2. Effect of Ech alone or in combination with TC-HT on the cell viability.** (A)
232 MTT viability assay of PANC-1 cells treated with different concentrations of Ech or in
233 combination with TC-HT treatment. (B) MTT viability assay of H6c7 normal human
234 pancreatic cells treated with 20 μM Ech or in combination with the same TC-HT
235 treatment. Data represent the mean ± standard deviation (n=3). Statistical significance
236 was determined by one-way ANOVA followed by Tukey's post-hoc test (***$P < 0.001$).
237
238 **Ech and TC-HT synergistically induce apoptosis in PANC-1 cells**
239 To confirm whether the decreased cell viability was associated with the induction of
240 apoptosis, flow cytometry with Annexin V-FITC and propidium iodide (PI) double
241 staining was performed. Annexin V is a phospholipid binding protein which has a
242 strong affinity for phosphatidylserine (PS) residues, and therefore can be used as a

243 probe for detecting apoptosis. PI, a membrane-impermeable nucleic acid dye, was used
244 to distinguish between the necrotic and apoptotic cells. The dot plot results (Fig 3A)
245 show a remarkable increase of apoptotic cell numbers (Q2+Q4) in the combination
246 treatment group. The bar graph (Fig 3B) shows that the average apoptotic rate of the
247 combination treatment group is significantly higher than that treated with Ech or TC-
248 HT alone. It demonstrated that co-treatment with TC-HT could synergize with Ech in
249 inhibiting the growth of PANC-1 cancer cells through inducing cell apoptosis.
250
251 **Fig 3. Assessment of the mode of cell death via Annexin V-FITC/PI double staining.**
252 (A) PANC-1 cells were treated with 20 μM Ech or in combination with TC-HT. After
253 24 h, the apoptotic state was assessed by flow cytometry with Annexin V/PI double
254 staining. (B) The quantified bar graph showed that the percentage of apoptotic cells
255 (Q2+Q4) was significantly higher in the combination treatment group. Data represent
256 the mean ± standard deviation (n=3). Statistical significance was determined by one-
257 way ANOVA followed by Tukey's post-hoc test (***$P < 0.001$).
258
259 **Ech and TC-HT synergistically decrease MTH1 and increase cellular ROS levels**
260 Previous study reported that Ech could serve as an MTH1 inhibitor by enzyme
261 catalyzed reaction [11]. In this study, we verify the effect of Ech treatment on MTH1
262 protein expression by Western blot analysis. As shown in Fig 4A, the Western blot result
263 demonstrated that 20 μM Ech treatment slightly reduced the MTH1 protein expression.
264 Moreover, we found that TC-HT alone significantly decreased the expression level of
265 MTH1 protein, while the combination of Ech and TC-TH further inhibited the
266 expression of MTH1 protein synergistically. In cancer cells, MTH1 is known as a key
267 factor for the remediation of ROS-mediated DNA damage caused by 8-oxo-dGTP.
268 To examine if cellular ROS level was affected by Ech and TC-HT co-treatment, the

269 fluorescent dye DHE was used to detect the ROS level. As it can be seen from Fig 4B
270 and 4C, treatment with Ech alone did not significantly increase the ROS level in PANC-
271 1 cells. On the other hand, the results showed that the treatment with TC-HT or the
272 combination treatment with Ech and TC-HT significantly increased the ROS level in
273 PANC-1 cells. In addition, it is noteworthy that the combination treatment (Ech + TC-
274 HT) induced the most significant ROS level elevation, which may result in a large
275 amount of DNA damage in cancer cells. The results suggest that Ech and TC-HT can
276 work synergistically to increase the cellular ROS level in PANC-1 cells, causing the 8-
277 oxo-dGTP accumulation to damage genomic DNA.
278
279 **Fig 4. Combined effect of Ech and TC-HT on MTH1 protein expression and ROS**
280 **level in PANC-1 cells. PANC-1 cells were treated with 20 μM Ech or in combination**
281 **with TC-HT. After 24 h, the MTH1 protein expression was quantified by Western**
282 **blot analysis and ROS level was assessed by flow cytometry.** (A) The MTH1 protein
283 expression was quantified and normalized to GAPDH internal control. (B) The ROS
284 level was assessed by DHE fluorescent dye, and the flow cytometry result was shown
285 as fluorescence intensity versus cell numbers. (C) The mean fluorescence intensity was
286 quantified as bar graph representing the ROS level. Data represent the mean ± standard
287 deviation (n=3). Statistical significance was determined by one-way ANOVA followed
288 by Tukey's post-hoc test (***$P < 0.001$).
289
290 **Ech and TC-HT synergistically increase accumulation of intracellular 8-oxo-**
291 **dGTP**
292 Since 8-oxo-dGTP is the major oxidized nucleotide inside cells, which tends to be
293 incorporated into DNA during replication, it leads to severe genome mutations and cell
294 death consequently. Cellular 8-oxo-dGTP is generated by ROS, therefore, increase in

295 cellular ROS would also result in increase in cellular 8-oxo-dGTP level. To directly
296 verify that more DNA mutants caused by 8-oxo-dGTP were accumulated in the cells by
297 the combination treatment (Ech + TC-HT), Alexa 488 was used to stain PANC-1 cells
298 after the treatment. Since avidin has been shown to bind to 8-oxo-dGTP with high
299 specificity, the DNA mispairing can thus be visualized by the green fluorescence in the
300 immunofluorescence images [14]. Fig 5A shows the immunofluorescence increased in
301 PANC-1 cells treated with 20 μM Ech or TC-HT for 24 hours, and significantly
302 increased in cells treated with the combination of TC-HT and 20 μM Ech. The
303 normalized RFU ratios of green/blue fluorescence (Fig 5B) reveal that cells treated with
304 the combination of Ech and TC-HT presented the highest 8-oxo-dGTP levels among
305 the four groups.
306
307 **Fig 5. Enhanced accumulation of 8-oxo-dGTP in PANC-1 cells with Ech and TC-**
308 **HT combination treatment. PANC-1 cells were treated with 20 μM Ech alone or in**
309 **combination with TC-HT. After 24 h, the fluorescent images were taken by an**
310 **inverted laser scanning confocal microscope.** (A) The confocal immunofluorescence
311 micrographs contained DAPI (blue), Alexa 488 (green), and the colocalization of both
312 stainings. The merged image shows Alexa 488 staining for DNA damage in green and
313 DAPI staining for nuclei in blue, indicating areas where DNA damage occurs within
314 the nuclei. Scale bar = 50 μm. (B) The 8-oxo-dGTP levels of cells were quantified by
315 calculating the normalized RFU ratio of green/blue fluorescence (Alexa 488/DAPI)
316 relative to the control group. Data represent the mean ± standard deviation (n=3).
317 Statistical significance was determined by one-way ANOVA followed by Tukey's post-
318 hoc test (***$P < 0.001$).
319
320 **TC-HT enhances the anticancer effect of Ech via modulating the MAPK family**

321 **proteins and inducing the apoptosis pathway in PANC-1 cells**

322 To further investigate the mechanism of TC-HT enhanced anticancer effect, the
323 expression levels of the MAPK family proteins and apoptosis-related proteins were
324 examined using Western blot analysis. There are three major subfamilies of MAPK
325 proteins which have been clearly characterized to play important role in cellular
326 functions: namely ERK, JNK, and p38 proteins [19]. The MAPK cascades are
327 responsible to relay, amplify and integrate extracellular signals to cellular responses
328 such as proliferation, differentiation, transformation, and apoptosis. It is known that
329 ERK proteins are important for cell survival and found to be upregulated in human
330 tumors, which led to the development of ERK inhibitors for cancer therapeutics [20].
331 JNK and p38, on the other hand, were deemed as stress responsive proteins and thus
332 involved in cell apoptosis [21]. Therefore, inhibition of ERK and concurrent activation
333 of JNK and p38 are critical for inducing apoptosis [22]. In this study, the results show
334 that p-JNK (Fig 6A) was strongly activated in the combination treatment of Ech and
335 TC-HT, while p-ERK (Fig 6B), on the other hand, was significantly inhibited. In
336 addition, the Bcl-2 family proteins are key regulators of the mitochondria pathway of
337 apoptosis, where the Bax/Bcl-2 ratio can be used to assess the upregulation of the
338 apoptotic signal. As shown in Fig 6C, we found that the Bax/Bcl-2 ratio was
339 significantly elevated in the combined treatment group, suggesting that TC-HT and Ech
340 could synergistically trigger the mitochondria-dependent apoptosis pathway. Moreover,
341 poly (ADP-ribose) polymerase (PARP) serves as an important nuclear enzyme in DNA
342 repairing. The cleavage of PARP by executioner caspases is the hallmark feature of
343 apoptosis, which leads to DNA damage. In this study, the cleaved PARP level was
344 examined by Western blot analysis. The results showed that co-treatment of Ech and
345 TC-HT greatly increased the expression of cleaved PARP proteins compared to the
346 control and single treatment groups (Fig 6D), indicating that the combination of Ech

347 and TC-HT synergistically activated caspase-dependent apoptosis pathway.

348

349 **Fig 6. Effect of Ech combined with TC-HT treatment on survival- and apoptosis-**
350 **related protein expressions in PANC-1 cells.** The experiments were conducted in
351 PANC-1 cancer cells treated with 20 μM Ech alone or in combination with TC-HT.
352 Western blot analyses of p-JNK (A), p-ERK and t-ERK (B), Bax and Bcl-2 (C), and
353 cleaved PARP (D) protein expressions. The expression levels of p-JNK and cleaved
354 PARP were normalized to GAPDH, and the p-ERK was normalized to t-ERK. Bax/Bcl-
355 2 ratio was calculated based on the Bax and Bcl-2 protein levels. Each relative
356 expression level was compared with control and represented as fold relative to control.
357 Data represent the mean ± standard deviation (n=3). Statistical significance was
358 determined by one-way ANOVA followed by Tukey's post-hoc test (***$P < 0.001$).

359

360 Discussion

361 With the aim of investigating the anticancer effect of Ech and TC-HT on PANC-1 cells,
362 the study finds that TC-HT strongly enhances the anticancer effect of Ech and causes
363 death of PANC-1 pancreatic cancer cells significantly. Previous studies have proven the
364 anticancer effect of Ech on some human cancer cell lines or animal models [23, 24].
365 Tang and co-workers, for instance, showed that Ech is capable of inhibiting breast
366 cancer cells by suppressing the Wnt signaling pathway [23]. Ye *et al*. demonstrated the
367 anticancer effects of Ech in HepG2 cells and mouse model [24]. With minimum harm
368 to normal cells and tissues, natural products are still unsuitable for direct anticancer
369 therapeutic application, due to insufficient efficacy and poor availability.

370 In this work, TC-HT was employed to significantly enhance the efficacy of natural
371 product Ech, exhibiting a synergistic effect inhibiting cancer cell growth and inducing

372 apoptotic cell death of PANC-1 pancreatic cancer cells. In the study, with only 20 μM
373 Ech in combination with TC-HT, one can achieve the same cell inhibition effect as at
374 100 μM Ech alone. That is to say the Ech dosage required to achieve effective anticancer
375 effect is greatly decreased to one fifth the original level, which also reduces damage to
376 healthy cells. Such result is inspiring because one can achieve the same anticancer
377 efficacy at much lower dosage. The enhanced specificity and efficacy of cancer
378 therapeutic modalities and reduced side effect could further improve the survival rate
379 of patients.

380 The study also finds that while TC-HT alone can suppress the expression level of
381 MTH1, its combination with Ech further increases the inhibitive effect on MTH1
382 expression. Some studies have manifested that Ech inhibits tumor growth by induction
383 of oxidative DNA damage or via specific signaling pathways [25-27]. One crucial
384 protein mediating the Ech-induced DNA damage is MTH1, which is responsible for
385 sanitizing oxidized dNTP pools to prevent incorporation of damaged bases during DNA
386 replication by, for example, converting 8-oxo-dGTP into 8-oxo-dGMP [28-30]. Gad *et*
387 *al*. showed that MTH1 is indispensable for cancer survival in several cancer cell lines
388 [14]. Moreover, previous study has reported that MTH1 depletion with interfering RNA
389 or small molecule inhibitors may cause DNA damage and apoptotic cell death in various
390 cancer cell lines [31]. Since then, a growing number of MTH1 inhibitors have been
391 developed in recent years [32-34]. Furthermore, recent studies have provided more
392 evidences that MTH1 inhibitors can delay tumor growth and inhibit metastasis both in
393 vitro and in vivo [35,36], further upholding their potential in cancer treatment.

394 Ech is one of a few natural products found to have inhibitive effect on MTH1 [37].
395 Dong *et al*. found that treatment of Ech inhibits MTH1 activity and increases DNA
396 damage marker, inducing apoptotic cell death and cell cycle arrest in human cancer cell
397 line, without harming normal cells [11]. Our study demonstrates that TC-HT application

398 significantly enhances Ech-induced MTH1 inhibition and DNA damage, as well as
399 apoptotic cell death, while slashing the viability of PANC-1 pancreatic cancer cells to
400 merely 20% of the control group. The outcome suggests that combined treatment has a
401 similar in vitro efficacy as chemotherapy drugs. Moreover, with the assistance of TC-
402 HT, it needs only 20 μM low dosage of Ech to attain the same cell inhibition efficacy
403 as at 100 μM Ech alone.

404 Through western blot analysis, the study attributes the enhanced anticancer effect
405 partially to the MTH1 protein inhibition triggered by the combination treatment. To the
406 best of our knowledge, this is the first study demonstrating that Ech suppresses the
407 MTH1 protein expression. The study also finds that TC-HT alone can effectively
408 suppress MTH1 expression, its combination with Ech greatly enhances the effect. The
409 DNA damage marker 8-oxo-dGTP also increases significantly in the combined
410 treatment group, confirming the linkage between abrogated MTH1 and DNA damage.
411 Dong *et al.* showed that Ech treatment could increase the cellular level of 8-oxo-dGTP,
412 but the ROS level remained unchanged after 24 h treatment of Ech [11], perhaps due to
413 the fact that Ech itself is also a potent antioxidant, thereby antagonizing the ROS level.
414 Since cellular 8-oxo-dGTP is also generated by ROS, increase in cellular ROS will
415 cause more 8-oxo-dGTP accumulation, creating more apoptotic signals. In the study,
416 with the assistance of TC-HT, we find that the combination treatment can significantly
417 increase not only 8-oxo-dGTP level but also ROS level, compared with Ech or TC-HT
418 treatment alone. Furthermore, many studies have demonstrated that ROS accumulation
419 could induce apoptosis by regulating the MAPK family protein expressions [38,39].

420 In our Western blot analysis, the results show that the combination treatment of
421 Ech and TC-HT strongly activates p-JNK, while significantly inhibiting p-ERK. The
422 combined treatment produces severe oxidative stress, which activates the apoptosis
423 signal through weakening cytoprotective p-ERK and activating stress-related p-JNK

424 proteins. In addition, the Bcl-2 family proteins play an important role in regulating
425 apoptosis and survival activities. Particularly, Bcl-2 protein, a key apoptosis-regulation
426 protein, is responsible for the sequestration of pro-apoptotic proteins such as Bax. It
427 binds to pro-apoptotic proteins to prevent the oligomerization and pore formation in the
428 mitochondrial membrane [40]. Moreover, it has been proven that Bcl-2 is a critical
429 apoptosis inhibitor which accounts for cancer chemoresistance [41,42]. Therefore,
430 several Bcl-2 inhibitors have been developed to target the Bcl-2 protein and found to
431 be synergistic with chemotherapeutic drugs [43,44]. In this study, the result shows that
432 the combination treatment significantly increases the Bax/Bcl-2 ratio, which primes
433 cancer cells for apoptosis via mitochondria-dependent apoptosis pathway. As the
434 anticancer mechanism triggered by the combination treatment is multipronged, the
435 synergistic effect is similar to combining MTH1, ERK, and Bcl-2 inhibitors, facilitating
436 the development of new anticancer drugs. Given the concern over their effect and
437 massive dosage in need, few herbal medicines have been applied in anticancer treatment.
438 In this work, our study proposes the application of TC-HT as a sensitizer, significantly
439 boosting the anticancer effect of Ech and thus slashing its dosage in need, facilitating
440 the application of Ech in cancer treatment.

441 In conclusion, combined TC-HT and Ech treatment targeting multiple pathways is
442 a novel cancer therapy with significant anticancer potential. The approach facilitates
443 apoptotic cell death in PANC-1 cancer cells via MTH1 inhibition, ROS and 8-oxo-
444 dGTP accumulations, and MAPK and Bcl-2 family protein regulations. Compared with
445 Ech administration alone, the co-treatment with TC-HT not only boosts a higher
446 efficacy treatment but also provides a safer and more comfortable medical procedure,
447 capable of contributing to the study of cancer treatment.

Funding

This work was supported by research grants from National Science and Technology Council (NSTC 112-2112-M-002-033 to CYC) and Ministry of Science and Technology (MOST 110-2112-M-002-004 and MOST 109-2112-M-002-004 to CYC) of the Republic of China. The funders had no role in study design, data collection and analysis, decision to publish, or preparation of the manuscript.

Competing Interests

The authors have declared that no competing interests exist.

Acknowledgments

The authors would like to acknowledge the Technology Commons in College of Life Science of National Taiwan University for use of flow cytometry system. We would also like to thank the Molecular Image Core Facility of National Taiwan Normal University under the auspices of the National Science and Technology Council for use of Laser Scanning Confocal Microscope System (ZEISS LSM880 with airyscan)/[BIO002514].

Author Contributions

Conceptualization: Chih-Yu Chao.

Data Curation: You-Ming Chen, Chih-Yu Chao.

Formal analysis: Wei-Ting Chen, You-Ming Chen, Guan-Bo Lin, Yu-Yi Kuo, Hsu-Hsiang Liu, Chih-Yu Chao.

Funding acquisition: Chih-Yu Chao.

Investigation: You-Ming Chen, Wei-Ting Chen, Chih-Yu Chao.

Supervision: Chih-Yu Chao.

Validation: You-Ming Chen, Wei-Ting Chen, Hsu-Hsiang Liu.

Writing – original draft: Wei-Ting Chen, You-Ming Chen, Chih-Yu Chao.

Writing – review & editing: Chih-Yu Chao.

References

1. Akhtar MF, Saleem A, Rasul A, Faran Ashraf Baig MM, Bin-Jumah M, Abdel Daim MM. Anticancer natural medicines: An overview of cell signaling and other targets of anticancer phytochemicals. Eur J Pharmacol. 2020; 888:173488.
2. Surh YJ. Cancer chemoprevention with dietary phytochemicals. Nat Rev Cancer. 2003; 3:768-780.
3. Zhu F, Du B, Xu B. Anti-inflammatory effects of phytochemicals from fruits, vegetables, and food legumes: A review. Crit Rev Food Sci Nutr. 2018; 58:1260-1270.
4. Biswas D, Nandy S, Mukherjee A, Pandey DK, Dey A. Moringa oleifera Lam. and derived phytochemicals as promising antiviral agents: A review. S Afr J Bot. 2020; 129:272-282.
5. Wang YH, Xuan ZH, Tian S, Du GH. Echinacoside protects against 6-hydroxydopamine-induced mitochondrial dysfunction and inflammatory responses in PC12 cells via reducing ROS production. Evid Based Complementary Altern Med. 2015; 2015:189239.
6. Geng X, Tian X, Tu P, Pu X. Neuroprotective effects of echinacoside in the mouse MPTP model of Parkinson's disease. Eur J Pharmacol. 2007; 564:66-74.
7. Wang N, Ji S, Zhang H, Mei S, Qiao L, Jin X. Herba Cistanches: Anti-aging. Aging Dis. 2017; 8:740-759.
8. Wei J, Zheng Z, Hou X, Jia F, Yuan Y, Yuan Y, et al. Echinacoside inhibits colorectal cancer metastasis via modulating the gut microbiota and suppressing the PI3K/AKT signaling pathway. J Ethnopharmacol. 2024; 318:116866.
9. Li W, Zhou J, Zhang Y, Zhang J, Li X, Yan Q, et al. Echinacoside exerts anti-tumor activity via the miR-503-3p/TGF-β1/Smad aixs in liver cancer. Cancer Cell Int. 2021;

502 21:304.
503 10. Shi Y, Cao H, Liu Z, Xi L, Dong C. Echinacoside Induces Mitochondria-Mediated
504 Pyroptosis through Raf/MEK/ERK Signaling in Non-Small Cell Lung Cancer Cells. J
505 Immunol Res. 2022; 2022:3351268.
506 11. Dong L, Wang H, Niu J, Zou M, Wu N, Yu D, et al. Echinacoside induces apoptotic
507 cancer cell death by inhibiting the nucleotide pool sanitizing enzyme MTH1. Onco
508 Targets Ther. 2015; 8:3649-3664.
509 12. Giribaldi MG, Munoz A, Halvorsen K, Patel A, Rai P. MTH1 expression is
510 required for effective transformation by oncogenic HRAS. Oncotarget. 2015. 6:11519-
511 11529.
512 13. Coskun E, Jaruga P, Jemth A-S, Loseva O, Scanlan LD, Tona A, et al. Addiction
513 to MTH1 protein results in intense expression in human breast cancer tissue as
514 measured by liquid chromatography-isotope-dilution tandem mass spectrometry. DNA
515 Repair. 2015; 33:101-110.
516 14. Gad H, Koolmeister T, Jemth AS, Eshtad S, Jacques SA, Ström CE, et al. MTH1
517 inhibition eradicates cancer by preventing sanitation of the dNTP pool. Nature. 2014;
518 508:215-221.
519 15. Zhou W, Ma L, Yang J, Qiao H, Li L, Guo Q, et al. Potent and specific MTH1
520 inhibitors targeting gastric cancer. Cell Death Dis. 2019; 10:434.
521 16. Hurwitz M, Stauffer P. Hyperthermia, radiation and chemotherapy: The role of
522 heat in multidisciplinary cancer care. Semin Oncol. 2014; 41:714-729.
523 17. Chen WT, Sun YK, Lu CH, Chao CY. Thermal cycling as a novel thermal therapy
524 to synergistically enhance the anticancer effect of propolis on PANC-1 cells. Int J Oncol.
525 2019; 55:617-628.
526 18. Lu CH, Chen WT, Hsieh CH, Kuo YY, Chao CY. Thermal cycling-hyperthermia
527 in combination with polyphenols, epigallocatechin gallate and chlorogenic acid, exerts
528 synergistic anticancer effect against human pancreatic cancer PANC-1 cells. PLoS One.
529 2019; 14:e0217676.
530 19. Ali ES, Akter S, Ramproshad S, Mondal B, Riaz TA, Islam MT, et al. Targeting
531 Ras-ERK cascade by bioactive natural products for potential treatment of cancer: an
532 updated overview. Cancer Cell Int. 2022; 22:246.
533 20. Cowan KJ, Storey KB (2003) Mitogen-activated protein kinases: new signaling
534 pathways functioning in cellular responses to environmental stress. J Exp Biol. 2003;
535 206:1107-1115.
536 21. Xiang Y, Ye W, Huang C, Lou B, Zhang J, Yu D, et al. Brusatol inhibits growth
537 and induces apoptosis in pancreatic cancer cells via JNK/p38 MAPK/NF-kb/Stat3/Bcl-
538 2 signaling pathway. Biochem Biophys Res Commun. 2017; 487:820-826.
539 22. Xia Z, Dickens M, Raingeaud J, Davis RJ, Greenberg ME. Opposing effects of

540 ERK and JNK-p38 MAP kinases on apoptosis. Science. 1995; 270:1326-1331.
541 23. Tang C, Gong L, lvzi X, Qiu K, Zhang Z, Wan L. Echinacoside inhibits breast
542 cancer cells by suppressing the Wnt/β-catenin signaling pathway. Biochem Biophys
543 Res Commun. 2020; 526:170-175.
544 24. Ye Y, Song Y, Zhuang J, Wang G, Ni J, Xia W. Anticancer effects of echinacoside
545 in hepatocellular carcinoma mouse model and HepG2 cells. J Cell Physiol. 2019;
546 234:1880-1888.
547 25. Wang W, Luo J, Liang Y, Li X. Echinacoside suppresses pancreatic
548 adenocarcinoma cell growth by inducing apoptosis via the mitogen-activated protein
549 kinase pathway. Mol Med Rep. 2016; 13:2613-2618.
550 26. Dong L, Yu D, Wu N, Wang H, Niu J, Wang Y, et al. Echinacoside induces
551 apoptosis in human SW480 colorectal cancer cells by induction of oxidative DNA
552 damages. Int J Mol Sci. 2015; 16:14655-14668.
553 27. Espinosa-Paredes DA, Cornejo-Garrido J, Moreno-Eutimio MA, Martínez-
554 Rodríguez OP, Jaramillo-Flores ME, Ordaz-Pichardo C. Echinacea Angustifolia DC
555 extract induces apoptosis and cell cycle arrest and synergizes with paclitaxel in the
556 MDA-MB-231 and MCF-7 human breast cancer cell lines. Nutr Cancer. 2020; 73:2287-
557 2305.
558 28. Sakumi K, Furuichi M, Tsuzuki T, Kakuma T, Kawabata S, Maki H, et al. Cloning
559 and expression of cDNA for a human enzyme that hydrolyzes 8-oxo-dGTP, a mutagenic
560 substrate for DNA synthesis. J Biol Chem. 1933; 268:23524-23530.
561 29. Oka S, Ohno M, Tsuchimoto D, Sakumi K, Furuichi M, Nakabeppu Y. Two distinct
562 pathways of cell death triggered by oxidative damage to nuclear and mitochondrial
563 DNAs. EMBO J. 2008; 27:421-432.
564 30. Ichikawa J, Tsuchimoto D, Oka S, Ohno M, Furuichi M, Sakumi K, et al.
565 Oxidation of mitochondrial deoxynucleotide pools by exposure to sodium nitroprusside
566 induces cell death. DNA Repair. 2008; 7:418-430.
567 31. Huber KVM, Salah E, Radic B, Gridling M, Elkins JM, Stukalov A, et al.
568 Stereospecific targeting of MTH1 by (S)-crizotinib as an anticancer strategy. Nature.
569 2014; 508:222-227.
570 32. Gao Y, Zhu L, Guo J, Yuan T, Wang L, Li H, et al. Farnesyl phenolic enantiomers
571 as natural MTH1 inhibitors from Ganoderma sinense. Oncotarget. 2017; 8:95865-
572 95879.
573 33. Yokoyama T, Kitakami R, Mizuguchi M. Discovery of a new class of MTH1
574 inhibitor by X-ray crystallographic screening. Eur J Med Chem. 2019; 167:153-160.
575 34. Streib M, Kräling K, Richter K, Xie X, Steuber H, Meggers E. An Organometallic
576 Inhibitor for the Human Repair Enzyme 7,8-Dihydro-8-oxoguanosine Triphosphatase.
577 Angew Chem Int Ed. 2014; 53:305-309.

578 35. Moukengue B, Brown HK, Charrier C, Battaglia S, Baud'huin M, Quillarda T, et
579 al. TH1579, MTH1 inhibitor, delays tumour growth and inhibits metastases
580 development in osteosarcoma model. EBioMedicine. 2020; 53:102704.
581 36. Zhan D, Zhang X, Li J, Ding X, Cui YX, Jia J. MTH1 inhibitor TH287 suppresses
582 gastric cancer development through the regulation of PI3K/AKT signaling. Cancer
583 Biother Radiopharm. 2020, 35:223-232.
584 37. Yin Y, Chen F. Targeting human MutT homolog 1 (MTH1) for cancer eradication:
585 current progress and perspectives. Acta Pharm Sin B. 2020; 10:2259-2271.
586 38. Lau ST, Lin ZX, Leung PS. Role of reactive oxygen species in brucein D-
587 mediated p38-mitogen-activated protein kinase and nuclear factor-kB signalling
588 pathways in human pancreatic adenocarcinoma cells. Br J Cancer. 2010; 102:583-593.
589 39. Li L, Yue GGL, Pu JX, Sun HD, Fung KP, Leung PC, et al. Eriocalyxin b-induced
590 apoptosis in pancreatic adenocarcinoma cells through thiol-containing antioxidant
591 systems and downstream signalling pathways. Curr Mol Med. 2014; 14:673-689.
592 40. Peng J, Ding J, Tan C, Baggenstoss B, Zhang Z, Lapolla SM, et al.
593 Oligomerization of membrane-bound Bcl-2 is involved in its pore formation induced
594 by tBid. Apoptosis. 2009; 14:1145-1153.
595 41. Dong J, Zhao YP, Zhou L, Zhang TP, Chen G. Bcl-2 upregulation induced by miR-
596 21 via a direct interaction is associated with apoptosis and chemoresistance in MIA
597 PaCa-2 pancreatic cancer cells. Arch Med Res. 2011; 42:8-14.
598 42. Cai BB, An Y, Lv N, Chen JM, Tu M, Sun J, Wei JS, Jiang KR, Miao Y. miRNA-
599 181b increases the sensitivity of pancreatic ductal adenocarcinoma cells to gemcitabine
600 in vitro and in nude mice by targeting Bcl-2. Oncol Rep. 2013; 29:1769-1776.
601 43. Zhao X, Sun W, Puszyk WM, Wallet S, Hochwald S, Robertson K, et al. Focal
602 adhesion kinase inhibitor PF573228 and death receptor 5 agonist lexatumumab
603 synergistically induce apoptosis in pancreatic carcinoma. Tumor Biol. 2017; 39:1-10.
604 44. Wang G, Chen S, Edwards H, Cui X, Cui L, Ge Y. Combination of chloroquine
605 and GX15-070 (obatoclax) results in synergistic cytotoxicity against pancreatic cancer
606 cells. Oncol Rep. 2014; 32:2789-2794.

Figure 1

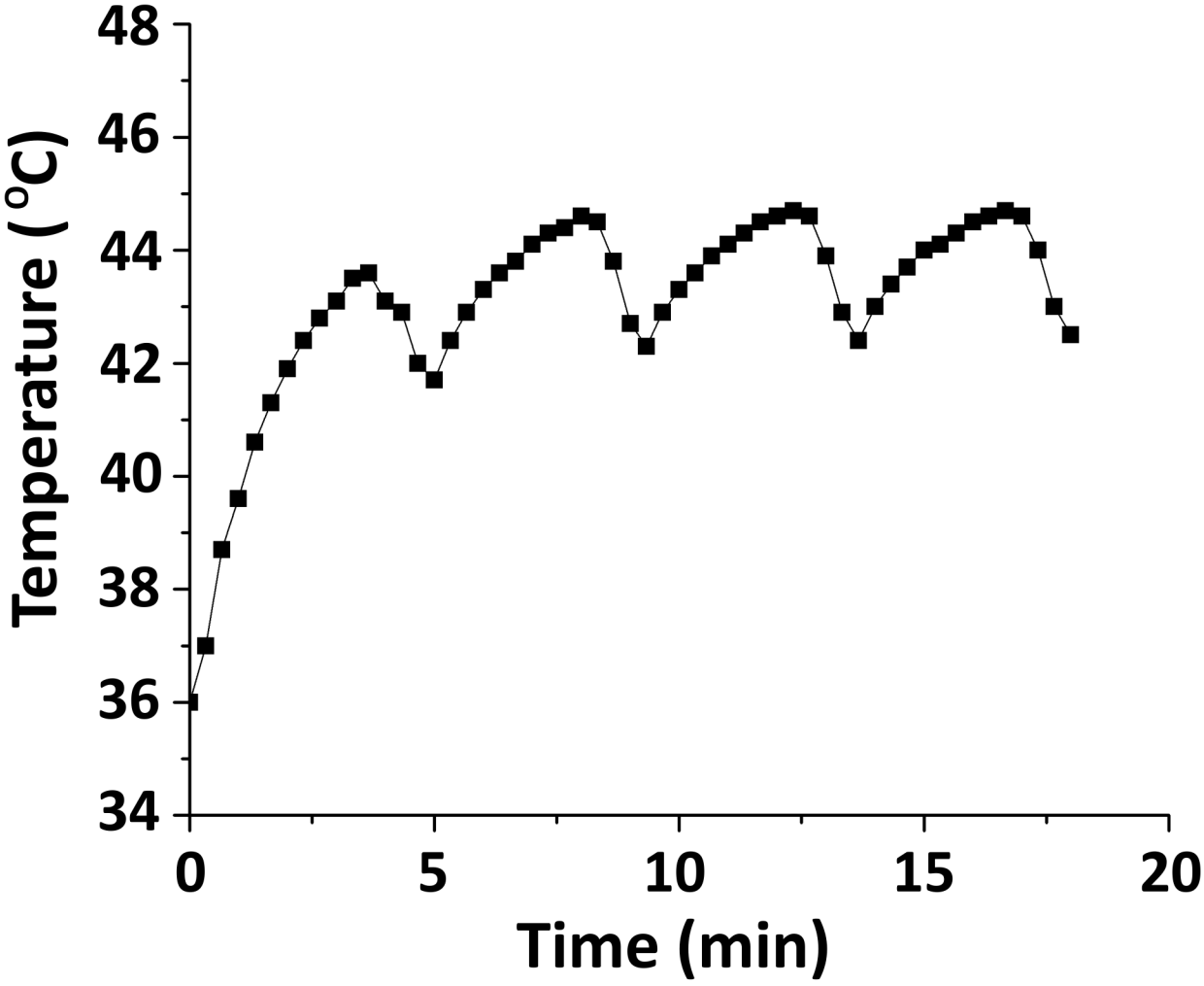

Figure 2

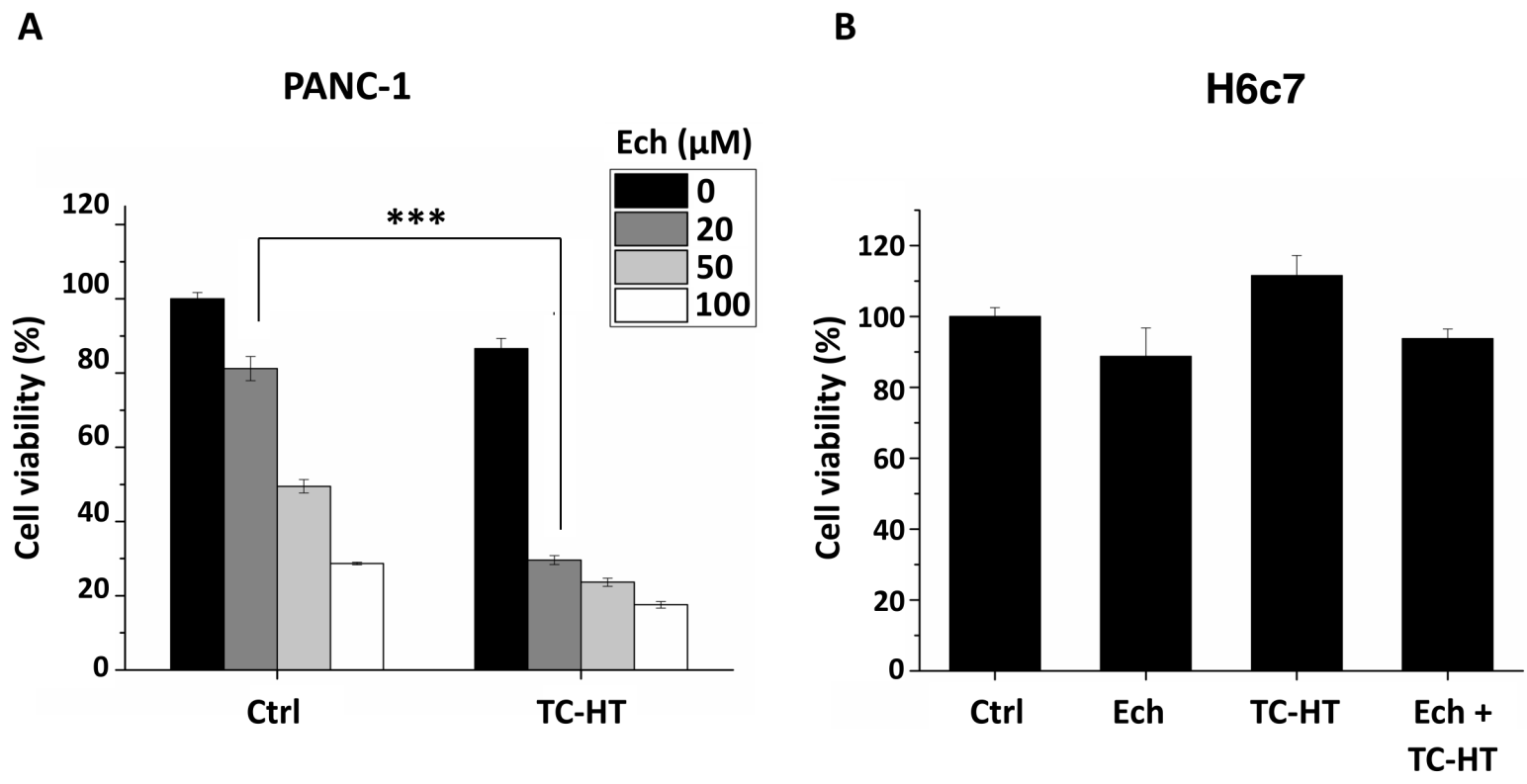
A
PANC-1
Ech (µM)
0
20
50
100
***
Cell viability (%)
120
100
80
60
40
20
0
Ctrl
TC-HT
B
H6c7
Cell viability (%)
120
100
80
60
40
20
0
Ctrl
Ech
TC-HT
Ech +
TC-HT

Figure 3

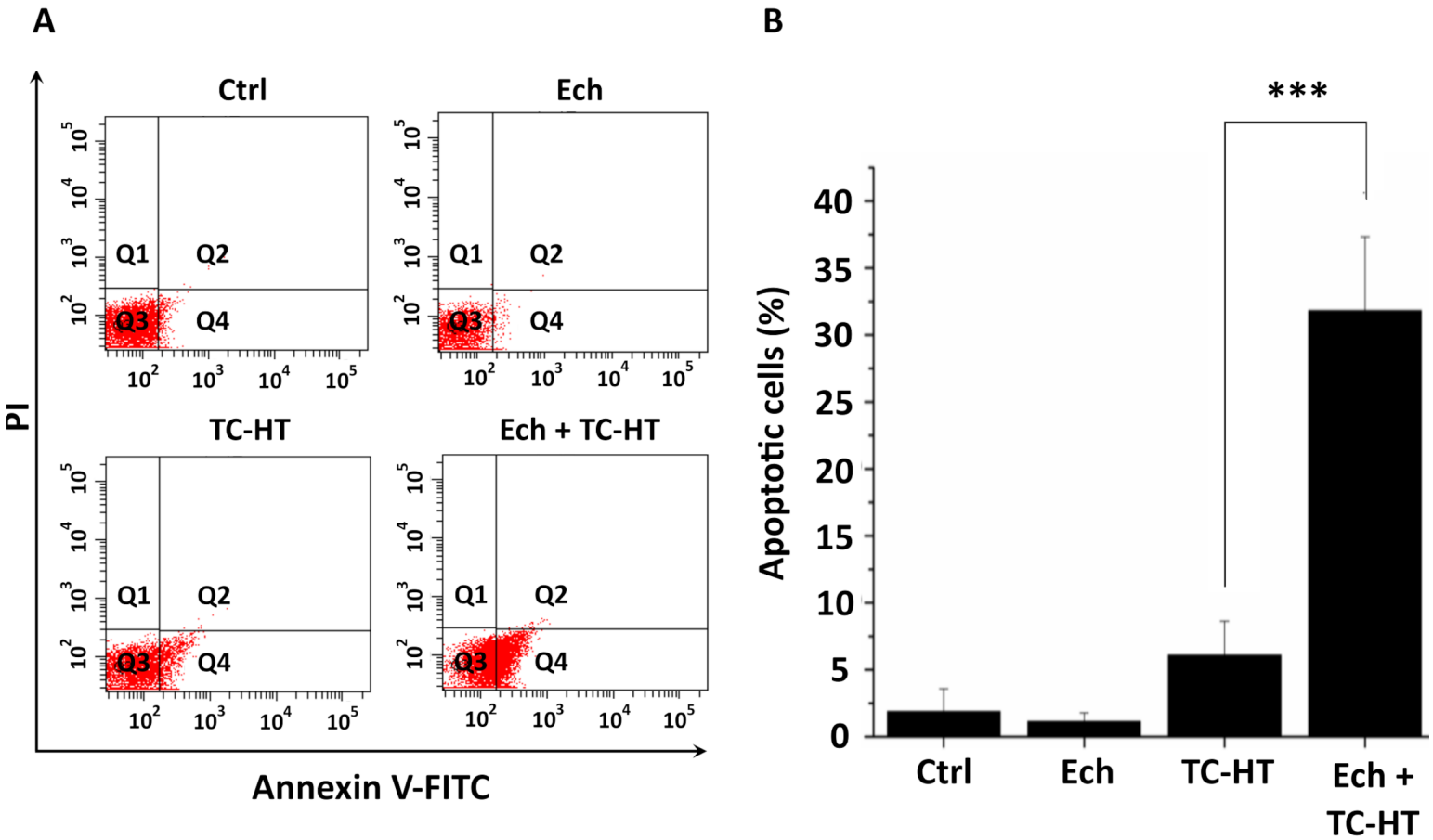
A
Ctrl
Ech
TC-HT
Ech + TC-HT
Q1
Q2
Q3
Q4
PI
Annexin V-FITC
B
***
Apoptotic cells (%)
0
5
10
15
20
25
30
35
40
Ctrl
Ech
TC-HT
Ech + TC-HT

Figure 4

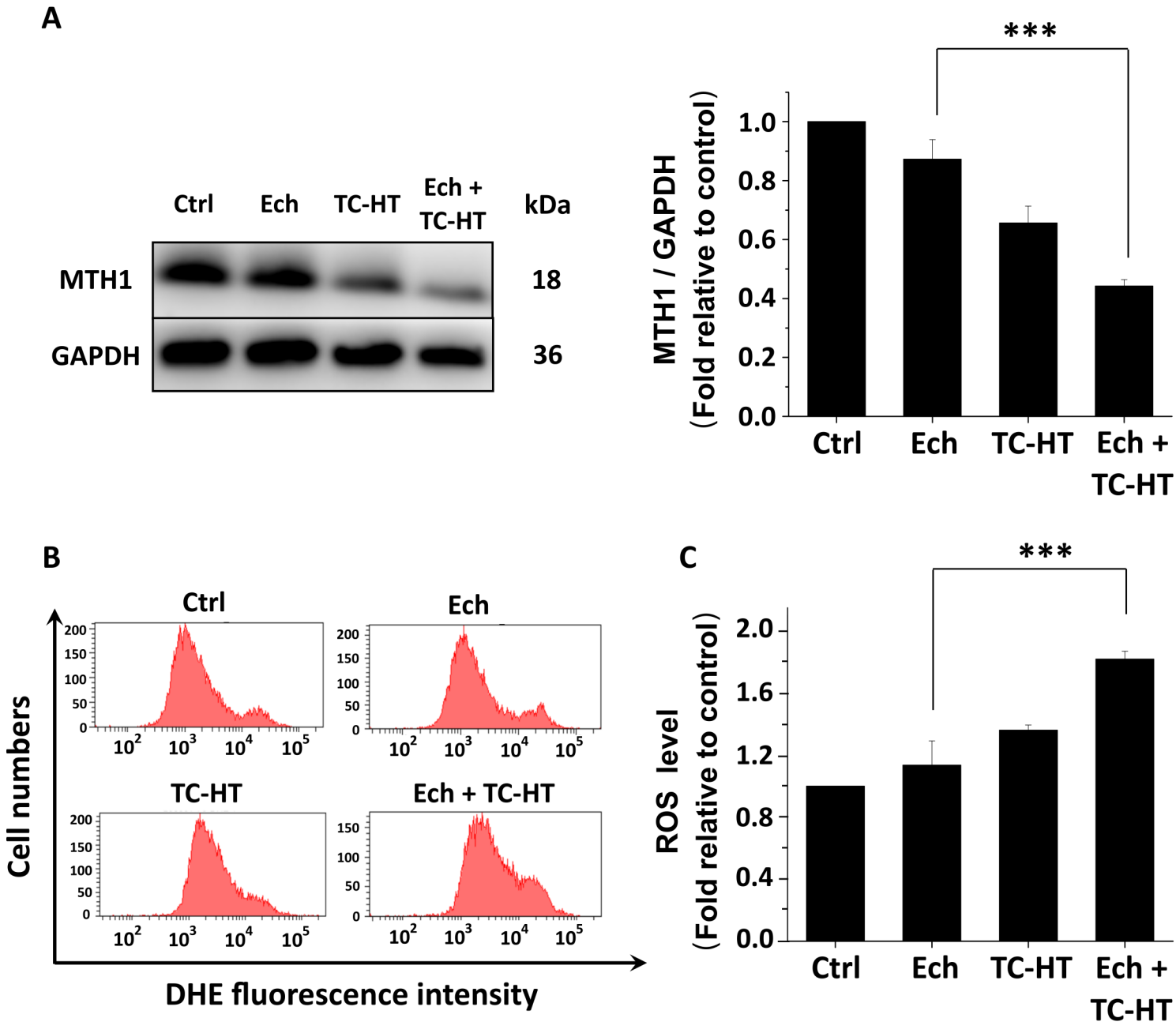
A
Ctrl
Ech
TC-HT
Ech + TC-HT
kDa
MTH1
18
GAPDH
36
***
MTH1 / GAPDH (Fold relative to control)
1.0
0.8
0.6
0.4
0.2
0.0
Ctrl
Ech
TC-HT
Ech + TC-HT
B
Ctrl
Ech
TC-HT
Ech + TC-HT
Cell numbers
DHE fluorescence intensity
C
***
ROS level (Fold relative to control)
2.0
1.6
1.2
0.8
0.4
0.0
Ctrl
Ech
TC-HT
Ech + TC-HT

Figure 5

A

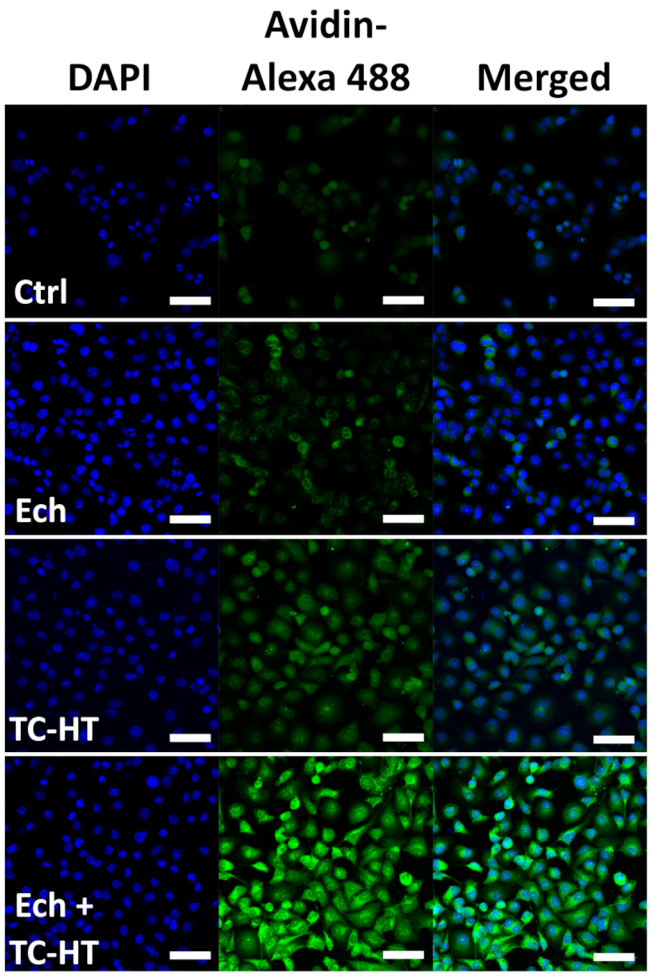
DAPI
Avidin-
Alexa 488
Merged
Ctrl
Ech
TC-HT
Ech +
TC-HT

B

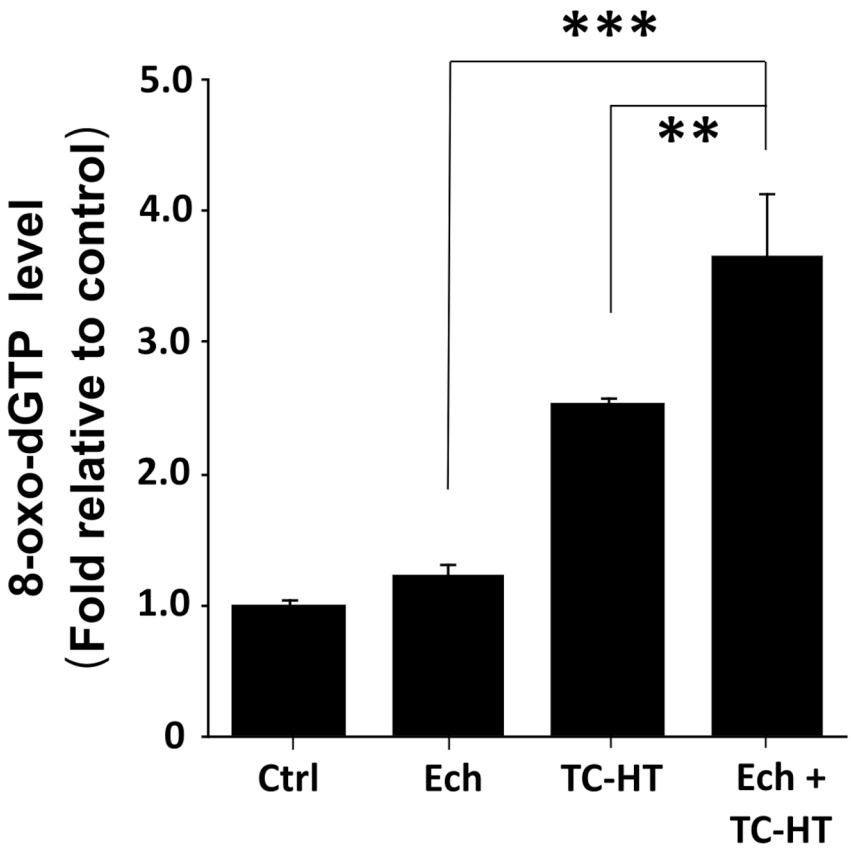
***
**
5.0
4.0
3.0
2.0
1.0
0
8-oxo-dGTP level
(Fold relative to control)
Ctrl
Ech
TC-HT
Ech +
TC-HT

Figure 6

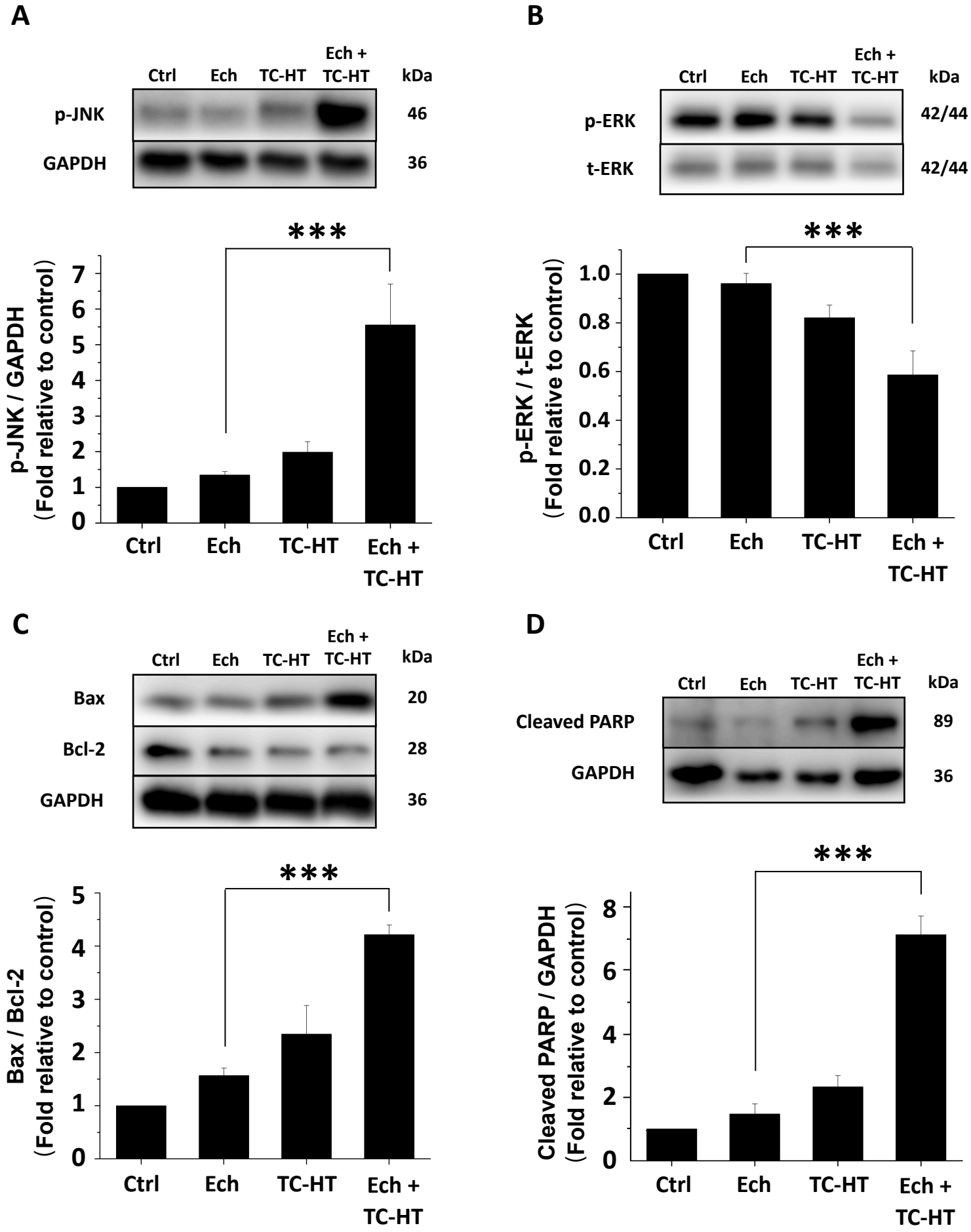
A
Ctrl
Ech
TC-HT
Ech + TC-HT
kDa
p-JNK
46
GAPDH
36
***
p-JNK / GAPDH (Fold relative to control)
0
1
2
3
4
5
6
7
Ctrl
Ech
TC-HT
Ech + TC-HT
B
Ctrl
Ech
TC-HT
Ech + TC-HT
kDa
p-ERK
42/44
t-ERK
42/44
***
p-ERK / t-ERK (Fold relative to control)
0.0
0.2
0.4
0.6
0.8
1.0
Ctrl
Ech
TC-HT
Ech + TC-HT
C
Ctrl
Ech
TC-HT
Ech + TC-HT
kDa
Bax
20
Bcl-2
28
GAPDH
36
***
Bax / Bcl-2 (Fold relative to control)
0
1
2
3
4
5
Ctrl
Ech
TC-HT
Ech + TC-HT
D
Ctrl
Ech
TC-HT
Ech + TC-HT
kDa
Cleaved PARP
89
GAPDH
36
***
Cleaved PARP / GAPDH (Fold relative to control)
0
2
4
6
8
Ctrl
Ech
TC-HT
Ech + TC-HT